A Water-Soluble pH-Responsive Molecular Brush of Poly(*N*,*N*-dimethylaminoethyl methacrylate) Grafted Polythiophene

Mingfeng Wang, Shan Zou, Gerald Guerin, Lei Shen, Kangqing Deng, Marcus Jones, Gilbert C. Walker, Gregory D. Scholes, and Mitchell A. Winnik*

Department of Chemistry, University of Toronto, 80 St. George Street, Toronto, M5S 3H6 Ontario, Canada

Received April 7, 2008; Revised Manuscript Received July 18, 2008

ABSTRACT: We report the synthesis of a new polythiophene (PT)-based molecular brush (PT-*g*-PDMA) by growing poly(*N,N*-dimethylaminoethyl methacrylate) (PDMA) chains from the PT backbone by ATRP. The polymer shows a reversible pH response in aqueous solution. A combination of AFM, light scattering, and ^{1}H NMR measurements indicated that the polymer brush forms a more extended conformation with a decrease in pH from 8 to 2 due to the protonation of the Me_2N- groups and increased repulsive interactions among the PDMA side chains, which drives the red shift of the absorption and PL spectra of the PT backbone. The good solubility of this polythiophene-based brush in a wide range of solvents is attractive for the fabrication of functional polymer composites.

Introduction

Conjugated polymers (CPs) are an important class of organic semiconductor materials. They serve as useful components of sensors[1] and optical/electrical devices such as polymer LEDs,[2] solar cells,[3] and transistors.[4] A prerequisite for these applications is the solubility and processability of the polymer, which was an early challenge in this field because of the limitations of most unsubstituted CPs. The conjugated backbone is typically rigid. The polymers tend to aggregate, resulting in poor solubility, low mechanical flexibility, and poor processability. One strategy to overcome this problem is to introduce flexible pendant groups along the conjugated backbone. These pendant groups not only can improve the solubility and processability of the CPs but also can provide sites where one can incorporate functional chemical or biological moieties.

Decoration of the conjugated backbone with alkyl chains renders the CPs soluble in common organic solvents, which leads to cost-effective fabrication of large-area thin films of CPs for devices based on a solution process. Recently, much attention has been turned to the synthesis of water-soluble CPs because of the increasing need to develop aqueous sensing systems and especially biological sensors.[5] A key advantage of CP-based sensors over small molecule analogues is their high sensitivity to minor perturbations due to the amplification by the collective response.[1] Both ionic and nonionic substituents have been attached to the conjugated backbone to achieve water solubility. Water-soluble CPs with nonionic groups such as oligoethylene oxides[6] and crown ethers[1] have been synthesized. These materials show solvato- and ionochromism. CPs with pendant ionic groups, also called conjugated polyelectrolytes, have been developed as highly sensitive fluorescence-based sensors for biological targets such as ATP and DNA as well as for temperature, solvent polarity, and pH.[7]

For example, Schanze et al.[8] reported a pH-responsive anionic poly(phenylene ethynylene) with pendant phosphonate groups. They observed a significant red shift of both the absorption and fluorescence (FL) spectra with a decrease of pH from 12 to 7.5, corresponding to the transition of the polymer from a relatively less aggregated or monomeric state at high pH to an aggregated state at low pH. More recently, Bazan et al.[9] reported a different kind of pH-responsive anionic conjugated polyelectrolyte containing substituted fluorine and phenylene units. The pendant groups of the phenylene units have carboxylic acid functionalities, which allow one to probe the effects of pH on optical properties. A decrease of pH gave rise to increased interchain contact, resulting in a red shift of the absorption maximum and a decrease of the PL efficiency. The aggregation of polymer chains at low pH was monitored by dynamic light scattering (DLS).

Despite the large number of applications of CPs in devices and sensors, the molecular mechanisms that drive the observed optical and electrochemical effects remain controversial or poorly understood. One reason is the difficulty of distinguishing conformational changes of individual molecules ("intrachain association") from intermolecular interactions (multimolecular aggregation).[7b,10] This state of affairs can be seen in the seemingly contradictory interpretations proposed for the solvatochromic behavior of different types of CPs. For instance, poly(3-alkoxy-4-methylthiophene) shows a red shift of the maximum of absorption from 425 nm in a good solvent (THF or $CHCl_3$) to 545 nm in a poor solvent (MeOH or EtOH).[7b] The color change for this polymer was attributed to a conformational transition of the polythiophene (PT) backbone. These authors proposed that in good solvents the PT chain exists as a disordered conformation with minimal electronic delocalization along the PT backbone and a shorter wavelength optical absorption; in contrast, an ordered backbone conformation in bad solvents leads to more extensive delocalization of the π-electrons and an optical absorption at a longer wavelength.

In contrast, different results were obtained for poly[2-methoxy-5-(2′-ethyl-hexyloxy)-1,4-phenylenevinylene] (MEH-PPV), and a different explanation was proposed.[11a] Both the absorption and PL spectra of MEH-PPV are slightly blue-shifted in THF (a poor solvent) relative to chlorobenzene (a good solvent). The blue shift of the spectrum in THF was attributed to a tighter conformation of the chain coil that forms in THF via twisting of the conjugated backbone, resulting in segments with a shorter effective conjugation length. A similar explanation was proposed for another conjugated polymer—poly[2,5-bis(*N*-methyl-*N*-hexylamino)phenylenevinylene] (BAMH-PPV).[11b,c] The amine groups along this polymer could be controllably protonated by addition of an organic acid, leading to a large blue shift of both the absorption and emission spectra. The authors propose that in nonpolar solvents the polymer chains collapse upon charging of a few percent of the side groups. The tight coiling of the polymer chain leads to a decrease in

* Corresponding author. E-mail: mwinnik@chem.utoronto.ca.

10.1021/ma800777m CCC: $40.75
Published on Web 09/04/2008

average conjugation length from the additional twisting of the backbone needed to fold the chain. Additional examples of how chain conformation and interchain interactions of CPs influence their optical and electrical properties can be found in recent reviews.[10−14]

A class of CP derivatives of particular interest to us is the CP-based molecular brush.[15−19] This term refers to molecules in which a second type of polymer, normally a flexible polymer, is grafted to the conjugated backbone. Several types of flexible polymers have been grafted along the conjugated backbone of CPs. These include poly(methyl acrylate),[15] polystyrene,[16] poly(ϵ-caprolactone) (PCL),[17] poly(*N*-isopropylacrylamide) (PNIPAAm),[18] and a more rigid polyquinoline.[19] These types of molecules offer several advantages over analogues containing small pendant moieties for experiments that establish a correlation between chain conformation or aggregation and the corresponding optical and electrical properties. First, the steric effect of the grafted polymer chains helps to segregate the conjugated polymer backbones from each other. Even when intermolecular aggregation takes place, it is more difficult for the conjugated polymer portions to come into contact. This feature makes it easier to distinguish intrachain conformational changes from interchain aggregation as the origin of shifts in the absorption and emission spectra. Second, repulsions among the polymer side chains leads to a more rigid and extended conjugated backbone. This factor also makes it possible to image the conformation of single molecules by atomic force microscopy (AFM).[20,21]

Another motivation for studying the correlation between chain conformation or aggregation of CP-brush copolymers and their optical and electrical properties is to find a way to induce or stimulate conformational transitions of the conjugated backbone, especially in a reversible manner. Very few stimuli-responsive CP-based molecular brushes have been synthesized for this purpose.[18] In this article we describe the synthesis, characterization, and properties of a new water-soluble and pH-responsive molecular brush with a polythiophene backbone and poly(*N,N*-dimethylaminoethyl methacrylate) (PDMA) side chains. This graft copolymer (noted as PT-*g*-PDMA) exhibits a reversible response to pH changes in water. By investigating the conformational transition of PT-*g*-PDMA associated with pH changes through DLS, AFM, and ^{1}H NMR measurements, we provide direct evidence for the molecular mechanism that drives the pH response of the polymer. We find that the extent of protonation of the PDMA side chains drives the extension and contraction of the PT conformational subunits, which, in turn, signals these changes through changes in the absorption and fluorescence spectra of the polymer solution.

Experimental Section

Materials and Methods. All chemicals were purchased from Aldrich and used as received. CH_2Cl_2 and $CHCl_3$ were dried by refluxing over CaH_2 followed by distillation. The pH of PT-*g*-PDMA solutions in water was adjusted with 1.0 M HCl or 1.0 M NaOH and recorded with a pH meter (PH/Mv/TEMP Meter P25, ROSE Scientific Ltd., Alberta).

Molecular Weight Measurements by GPC. The apparent molecular weights of the polythiophene macroinitiator and the polymer brush were measured by gel permeation chromatography (GPC) with linear polystyrene samples as molar mass standards. The GPC employing either *N*-methylpyrrolidone (NMP) or THF with triethylamine (Et_3N) (2.0 vol %) as the eluent was equipped with a Viscotek model 3210 UV/vis detector and a Viscotek model 3580 differential refractive index (RI) detector. The wavelength of the UV/vis detector was set at 420 nm. The GPC running pure THF as the eluent was a Viscotek TDA302 system integrated with a triple detector array featuring a low angle light scattering (LALS) detector, a four-capillary differential viscometer, and an RI detector. The flow rate for each GPC was 0.6 mL/min.

Spectroscopic Measurements. UV−vis absorption spectra were collected on a Perkin-Elmer Lambda 25 spectrometer using 1.00 cm quartz cuvettes. Fluorescence (FL) spectra were measured using a SPEX Fluorolog-3 spectrofluorometer (Jobin Yvon/SPEX, Edison, NJ). The temperature-dependent FL spectra were measured using a temperature-controlled cuvette holder connected to a bath circulator (NESLAB RTE111), with a temperature precision of ±0.01 °C. ^{1}H NMR spectra were recorded at 400 MHz using a Varian Mercury spectrometer. Fluorescence decay profiles were measured by time-correlated single photon counting,[22] using picosecond excitation pulses from a Spectra-Physics MillenniaXs-P Ti−sapphire laser, pumped with a solid-state diode laser emitting at 532 nm. A picosecond pulse selector and a frequency doubler were used in order to adjust the repetition rate of the laser to ca. 8 MHz and the wavelength to 450 nm. The data were analyzed using a least-squares fitting algorithm involving the iterative reconvolution of a model exponential decay function with the measured instrument response function. The short time resolution of the instrument is ~30 ps (~15% fwhm of the instrument response). The samples were degassed by freeze−pump−thaw (five cycles) before the measurement and sealed in Pyrex tubes (o.d. = 1 cm).

AFM Measurements. AFM measurements were taken on a Digital Instruments Dimension 5000 AFM with a Nanoscope IIIa controller (DI/Veeco, Santa Barbara, CA) operated in the tapping mode using silicon probes (Mikromasch USA, resonance frequencies in the range of 175−350 kHz, free amplitude: 20−25 nm) at RT. One drop of dilute solution of polymer (2×10^{-3} g/L) in toluene, THF, CH_2Cl_2, or water (at different pH) was placed onto freshly cleaved mica surfaces and dried at ambient temperature.

d*n*/d*c* Measurements. The refractive index increment (d*n*/d*c*) of the polythiophene macroinitiator (PEBBT) in THF was determined by a chromatographic method. Three solutions in THF with different known concentrations (0.655, 1.035, and 1.548 mg/mL) of polymer were injected into the GPC with the triple detector array. The injection volume (V_{inj}) was fixed at (100 μL). We calculated a value of d*n*/d*c* = 0.18 mL/g from a plot of the RI peak area (RI_{area}) vs sample concentration (c_S), in accord with the expression

$$RI_{area} = \Delta V_i \sum_i RI_i = \frac{RI_{cal}}{n_0} \frac{dn}{dc} c_S V_{inj} \quad (1)$$

where n_0 is the refractive index of the solvent (THF), and RI_{cal} is the detector calibration factor.

The d*n*/d*c* of the PT-*g*-PDMA brush in THF was 0.090 mL/g, as measured at a wavelength of 620 nm using a BI-DNDCW differential refractometer from Brookhaven Instruments Co. (Holtsville, NY). The refractometer was first calibrated with solutions of poly(methyl methacrylate) (PMMA) (M_p = 107 000 g/mol, M_w/M_n = 1.1, Polymer Laboratories Ltd., Amherst, MA) in THF. The d*n*/d*c* of PMMA in THF at 30 °C is 0.0877 mL/g.

Light Scattering Measurements. Static (SLS) and dynamic light scattering (DLS) measurements were performed using a wide angle light scattering photometer from ALV. The light source was a JDS Uniphase He−Ne laser (λ_0 = 632.8 nm, 35 mW) emitting vertically polarized light. The cells were placed into the ALV/DLS/SLS-5000 compact goniometer system and sat in a vat of *cis*-decahydronaphthalene, which matched the index of refraction of the glass cells. The scattered light was detected by a Dual ALV-High Q.E. APD avalanche photodiode module, interfaced to the ALV-5000/EPP multiple tau digital. All measurements were carried out at room temperature. SLS and DLS experiments were performed simultaneously. The angular range consisted of scattering angles between 30° and 150° (at 5° intervals). Toluene was used as the standard in the SLS measurements.

Synthesis of 3-[1-Ethyl-2(2-bromoisobutyrate)]thiophene (EBBT). 3-Thiophene−ethanol (2.5 g, 19.5 mmol) and triethylamine (2.2 g, 21.7 mmol) were dissolved in 35 mL of anhydrous CH_2Cl_2 in a 250 mL three-neck round-bottom flask. The mixture was stirred under a N_2 atmosphere and cooled in an ice/water bath

to 0 °C. Then 2-bromoisobutyryl bromide (4.9 g, 21.4 mmol) was dissolved in 10 mL of CH_2Cl_2. The solution was transferred into a 25 mL pressure-equalizing funnel and added dropwise into the flask over 0.5 h under stirring. After complete addition, the reaction mixture was warmed to room temperature and kept stirring for 24 h. The triethylamine hydrochloride salt precipitating from the mixture was filtered after the reaction. The filtrate was diluted to ca. 50 mL with CH_2Cl_2 and washed in turn with 1% HCl, saturated $NaHCO_3$, saturated NaCl, and distilled water (ca. 50 mL for each solution). The organic layer was collected and dried with anhydrous $MgSO_4$ overnight. The product was further purified by a silica column chromatography in a solvent mixture of hexane/ethyl acetate (95/5, v/v). The final product was dried under vacuum, and a brown liquid was obtained. Yield: 3.5 g (65%).

Synthesis of 2,5-Poly(3-[1-ethyl-2(2-bromoisobutyrate)]thiophene) (PEBBT). Anhydrous $FeCl_3$ (2.5 g, 15 mmol) was dispersed into 20 mL of anhydrous $CHCl_3$ in a 100 mL round-bottom flask. Then EBBT (1.0 g, 3.6 mmol) was dissolved in 20 mL of $CHCl_3$ in a 25 mL pressure-equalizing funnel and added dropwise into the flask under stirring over 20 min. After stirring the mixture at room temperature for 2 days, it was added dropwise into 1.2 L methanol and stirred for another 2 h. The solid was collected on a Büchner funnel with filter paper and washed with methanol four times. The resulting precipitate was Soxhlet extracted with methanol for 2 days and then dried under vacuum at room temperature overnight. The dark brown powder obtained was dissolved and refluxed in a mixture of 120 mL of $CHCl_3$ and 100 mL of concentrated ammonia for 2 days to remove the $FeCl_3$ remaining in the polymer product. The $CHCl_3$ layer was separated and collected. The solution was concentrated by removal of some solvent under rotary evaporation and precipitated in 100 mL of methanol. The red precipitate was washed three times with methanol and dried under vacuum at room temperature overnight. For this polymer (GPC: THF+2.0 vol % Et_3N), $M_n = 44\,000$ and $M_w/M_n = 8.2$. The polymer was then fractionated by preparative size exclusion column chromatography using a column packed with TOYOPEARL gel (HW-65F from TOSOH, Japan) with THF as the eluent.

Synthesis of 2,5-Poly(3-[1-ethyl-2(2-(poly(*N,N*-dimethylaminoethyl methacrylate))]thiophene) (PT-*g*-PDMA). In a 100 mL Schlenck flask (flask A), a fractionated PEBBT (54 mg, 0.2 mmol Br, $M_n = 1.9 \times 10^5$, $M_w/M_n = 1.9$) was dissolved in 6 mL of anisole. Then $CuBr_2$ (1.2 mg, 5.0×10^{-3} mmol) was added. The mixture was deoxygenated by three cycles of freeze−pump−thaw. In another 50 mL round-bottom flask (flask B), $CuBr_2$ (1.2 mg, 5.0×10^{-3} mmol), CuBr (14 mg, 0.1 mmol), and 1,1,4,7,10,10-hexamethyltriethylenetetramine (58 mg, 0.25 mmol) were charged, and then *N,N*-dimethylaminoethyl methacrylate (DMA, 7.4 g, 47.1 mmol, purified by passing through a silica column) was added to flask B. The mixture was deoxygenated by N_2 bubbling for at least 1 h. Then the mixture in flask B was transferred into flask A with a two-ended needle under N_2 protection. Then flask A was deoxygenated by three cycles of freeze−pump−thaw and was placed in a thermostated oil bath at 80 °C and stirred for 1.5 h. The polymerization was stopped by cooling the mixture to room temperature and exposing the mixture to air. The mixture was diluted with 100 mL of THF and passed through an alumina column to remove the copper catalyst. The THF solution was concentrated by removing some solvent under vacuum and precipitated in 200 mL of hexane. The supernatant was decanted. The viscous precipitate was redissolved in ca. 5 mL of THF and precipitated in 200 mL of hexane. The precipitation process was repeated again, and the polymer product was dried in vacuum oven at 30 °C overnight. Yield: 2.1 g (28% based upon DMA). The weight ratio of the polythiophene backbone in the final product was 2.6% if all the macroinitiator was assumed to be reacted completely.

UV−Vis Absorption Measurements. A solution of PEBBT was prepared by dissolving the polymer solid (0.37 mg) into a weighed amount of THF (4722.3 mg, 5.306 mL). This solution was then diluted with THF (by weighing) to obtain four samples with polymer concentrations $c = 1.85$, 3.40, 6.34, and 11.9 μg/mL.

Scheme 1. Synthetic Route to PT-*g*-PDMA

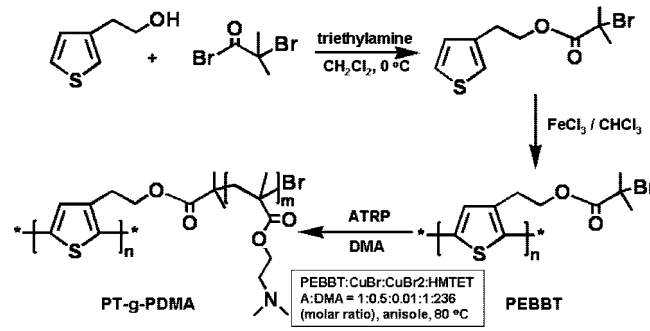

Table 1. Molecular Weight Characterization by GPC

polymer	$10^{-6}M_n$	M_w/M_n	$10^{-6}M_n$	M_w/M_n
PEBBT	0.20[a]	1.6[a]	0.19[b]	1.9[b]
PT-*g*-PDMA	—[a,d]	—[a,d]	0.59[c]	3.9[c]

[a] From GPC running in NMP and polystyrene standards. [b] From GPC (equipped with a triple detector array) running in THF, using $dn/dc = 0.18$ determined independently. [c] From GPC running in THF/$N(Et)_3$ (2 vol %) and polystyrene standards. In the absence of $N(Et)_3$, the polymer does not elute from the column. [d] Part of the sample exceeds the molecular weight cutoff of the column.

Solutions of PT-*g*-PDMA with four different concentrations ($c =$ 0.055, 0.140, 0.264, and 0.444 mg/mL) were prepared by weighing out individual samples of polymer on a microbalance and dissolving them into known weights of THF. Beer−Lambert plots were constructed of the maximum absorbances of PEBBT (at 423 nm) and PT-*g*-PDMA (at 435 nm) against the weight concentrations of each polymer, from which we calculated "extinction coefficient" values of $\varepsilon_{423\ nm} = 23.3$ mL mg^{-1} cm^{-1} for PEBBT at 423 nm and $\varepsilon_{435\ nm} = 0.69$ mL mg^{-1} cm^{-1} for PT-*g*-PDMA.

Effect of Light Exposure on the Stability of PT-*g*-PDMA in THF. To test for polymer degradation, a sample of PT-*g*-PDMA was dissolved in THF along with a sample of polystyrene ($M_n =$ 15 800, PDI = 1.05) as an internal standard. After filtration (0.2 μm filter), one part of the solution was exposed to room light while another part was kept in dark. Aliquots of these solutions were taken over time and analyzed by GPC (THF+2.0 vol % Et_3N).

Results and Discussion

Polymer Synthesis and Characterization. The synthesis route to the PT-*g*-PDMA polymer brush is presented in Scheme 1. We synthesized PT-*g*-PDMA by atom-transfer radical polymerization (ATRP) of *N,N*-dimethylaminoethyl methacrylate (DMA) initiated by the pendant groups of a macroinitiator (PEBBT) prepared by oxidative polymerization of 3-[1-ethyl-2-(2-bromoisobutyrate)]thiophene (EBBT) with $FeCl_3$ in chloroform. PEBBT was fractionated by preparative size-exclusion chromatography to obtain a sample with a much narrower molecular weight distribution. This sample was initially characterized by GPC in NMP using polystyrene standards to obtain a molecular weight ($M_n = 200\,000$, $M_w/M_n = 1.6$; see Table 1). To obtain a more accurate value, we redetermined the molecular weight by GPC in THF using the triple detector in conjunction with an independently measured value of $dn/dc =$ 0.18 mL/g. In this way, we obtained $M_n = 190\,000$ ($M_w/M_n =$ 1.9), corresponding to a degree of polymerization of 690. These values are very similar. This concordance of these values may not be accidental. Heffner et al.[27] compared the apparent molecular weights of poly(3-hexylthiophene) samples determined by GPC with the absolute values determined by light scattering and viscosity measurements and found reasonable agreement.

After the ATRP polymerization step, the polymer peak in the NMP GPC trace (Figure 1) was shifted to a much smaller

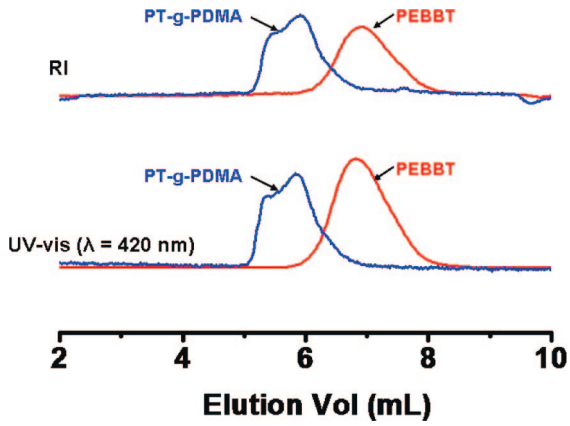

Figure 1. GPC traces of PEBBT macroinitiator and PT-*g*-PDMA. Solvent: *N*-methyl-2-pyrrolidinone; flow rate: 0.6 mL/min.

elution volume. One also sees two peaks in the refractive index (RI) trace and in the UV−vis trace, a consequence of the fact that the molecular weight of the polymer brush exceeds the cutoff of the GPC column. Figure 2 presents ^{1}H NMR spectra of the thiophene monomer EBBT, the polythiophene macroinitiator PEBBT, and the final polymer brush. All the peaks of EBBT became broader after its polymerization. The splitting of the peaks d and e at 3 and 4.4 ppm, respectively, into two components is an indication of heterogeneous monomer addition, i.e., head-to-tail, head-to-head, and tail-to-tail.[23] The amount of head-to-tail coupling is ca. 60%. After the growth of the PDMA side chains by ATRP, all of the peaks of the PDMA protons appeared in the ^{1}H NMR spectrum, whereas the signals of the PT backbone could not be observed. We attribute the absence of PT signals to two factors. First, there are relatively few protons on the thiophene rings compared to the much greater number of protons on the PDMA side chains. In addition, restricted mobility may also lead to peak broadening, making small peaks from the PT protons even more difficult to discern. A similar phenomena was observed by Müller et al.[24] in the ^{1}H NMR spectra of poly(2-(2-bromoisobutyloxy)ethyl methacrylate) brushes with poly(*tert*-butyl acrylate)-*b*-poly(styrene) as side chains.

The unfortunate consequence of the lack of polythiophene signals in the NMR is that we cannot use NMR to determine the composition of the graft copolymer. On the basis of the amount of PEBBT used as initiator and the weight of polymer obtained as the product, we estimate that the graft copolymer contains 97.4 wt % PDMA and 2.6 wt % PT. GPC measurements in NMP solution were unable to provide meaningful molecular weight values because the sample exceeded the molar mass cutoff of the column. The polymer did not elute from a GPC column packed in THF, and in a THF−2 wt % Et_3N mixture, the polymer appeared to have its elution retarded by adsorption to the column. Light scattering measurements on solutions of the polymer in THF were complicated by the presence of a small fraction of aggregates that could not be removed by filtration, making it impossible to obtain a reliable Zimm plot. In an attempt to obtain independent information about the PT content of the block copolymer, we measured the absorbance values at λ_{max} for solutions of PEBBT (λ_{max} = 423 nm) and of PT-*g*-PDMA (λ_{max} = 435 nm) at various concentrations in THF. From plots of absorbance vs concentration and the assumption that the extinction coefficients per thiophene unit of the two polymers are similar, we calculate a polymer composition of 3.0 wt % PT. There is an uncertainty in this analysis because the absorption spectrum of polythiophene is sensitive to its conformation (i.e., to the distribution of conjugation lengths). Nevertheless, we take the agreement between this result and that based on the mass yield of polymer to indicate that the graft copolymer contains ~97 wt % PDMA, implying that the number-average degree of polymerization of each arm of the PDMA brush is 60.

The PT-*g*-PDMA polymer had a T_g of 20 °C as measured by differential scanning calorimetry (DSC). It shows high solubility in a wide range of solvents such as toluene, THF, chloroform, CH_2Cl_2, methanol, *N*-methyl-2-pyrrolidinone, and water (Figure S1, Supporting Information), reflecting the solubility of the PDMA side chains in these solvents. PDMA itself is a pH-sensitive polymer, which is cationic when protonated.[25,26] The reported pK_a of PDMA homopolymer in water is ca. 7.5 and varies a little (±0.3) with molecular weight.[25] The solubility of PDMA in water is dependent on pH and temperature. For instance, the polymer is very soluble at low pH (e.g., 4) at room temperature but not soluble at pH 12 at 65 °C.[26] In the following section, we discuss how the optical properties of the PT backbone are influenced by changes in solvent polarity and by pH changes in water.

Photostability of PT-*g*-PDMA. In 1991, Heffner et al.[27] reported that poly(3-hexylthiophene) (P3HT) in solution in $CHCl_3$ or THF degraded upon exposure to light. We tested the stability of THF solutions of PT-*g*-PDMA upon exposure to room light. A solution of the polymer in THF was prepared along with a polystyrene sample (M_n = 15 800, PDI = 1.05) as an internal standard, which was assumed to be inert. One part of the solution was exposed to room light over 49 h, while another part was kept in the dark. GPC results (Figure S2, Supporting Information) indicated that no change occurred for the sample kept in dark. In contrast, the elution peak of PT-*g*-PDMA from the solution exposed to room light decreased in intensity with the increase of exposure time and eventually disappeared. Unexpectedly, no new peak appeared in the low molecular weight range. Furthermore, the ^{1}H NMR and UV−vis absorption spectra of the solution exposed to light remained unchanged, as did those of the sample kept in dark. These results imply that the polymer brush is sensitive to light, and small extents of reaction may form products that stick to the GPC column. The underlying mechanism of the photochemical change is not clear. As a consequence of these results, we took precautions to minimize sample exposure to room light.

Factors Affecting the Optical Properties of PT-*g*-PDMA in Solution. *Solvochromic and pH Effects.* Figure 3a−d shows the absorption and emission spectra of PEBBT macroinitiator in THF as well as PT-*g*-PDMA in THF and in water at different pH values. Figure 3e shows the time-resolved fluorescence (FL) spectra of these samples. In each sample the PL decay profile was nonexponential but could be fitted to a biexponential decay function: $I(t) = \alpha_1(\exp(-t/\tau_1) + \alpha_2(\exp(-t/\tau_2)$ with fitted values in the range 240 ps < τ_1 < 340 ps and 540 ps < τ_2 < 600 ps. For the PEBBT macroinitiator in THF, the wavelengths of the maximal absorbance ($\lambda_{max,abs}$) and emission ($\lambda_{max,em}$) are 423 and 552 nm, respectively. After the growth of the PDMA side chains, there was a red shift (ca. 10 nm) of $\lambda_{max,abs}$ and a blue shift (ca. 6 nm) of $\lambda_{max,em}$ in THF, accompanied by a decrease of the average FL lifetime from 585 ps (PEBBT) to 513 ps (PT-*g*-PDMA). The measured Stokes shift is larger for the PEBBT macroinitiator than for the PDMA-substituted polymers. This difference could arise from a greater flexibility of the polythiophene backbone in the absence of PDMA side chains, which might facilitate larger excitonic structural distortions relative to the PEBBT ground state: i.e., exciton−phonon coupling strength is larger in bare PEBBT polymer. The absorption and emission spectra of PT-*g*-PDMA were very similar in all of the organic solvents tested such as toluene, CH_2Cl_2, THF, $CHCl_3$, and methanol. While the polymer in water (pH 8) showed little shift for $\lambda_{max,abs}$ in comparison with the

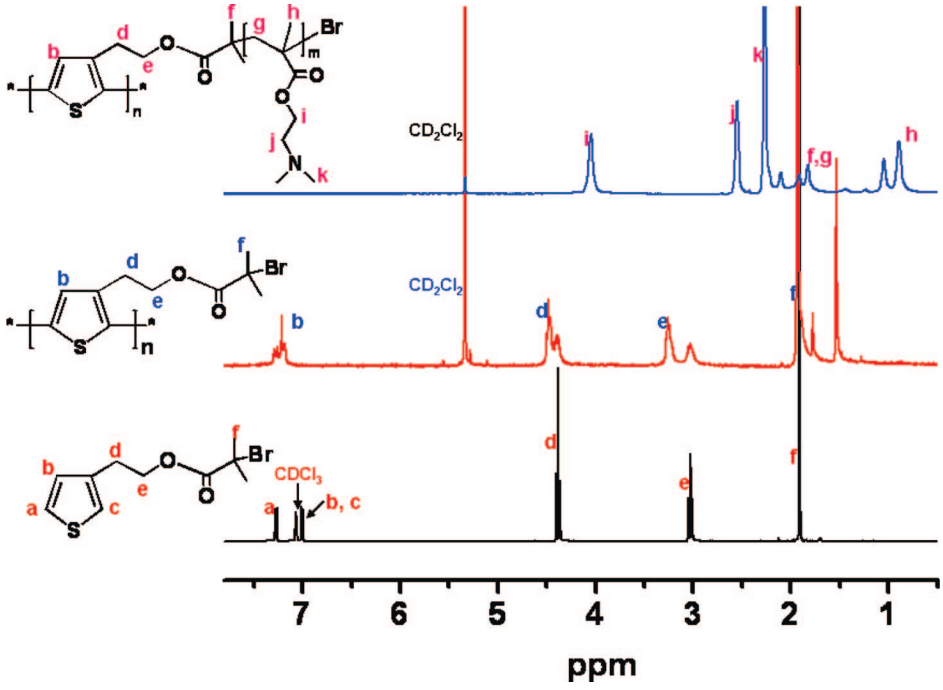

Figure 2. ^{1}H NMR spectra of EBBT ($CDCl_3$), PEBBT (CD_2Cl_2) and PT-*g*-PDMA (CD_2Cl_2).

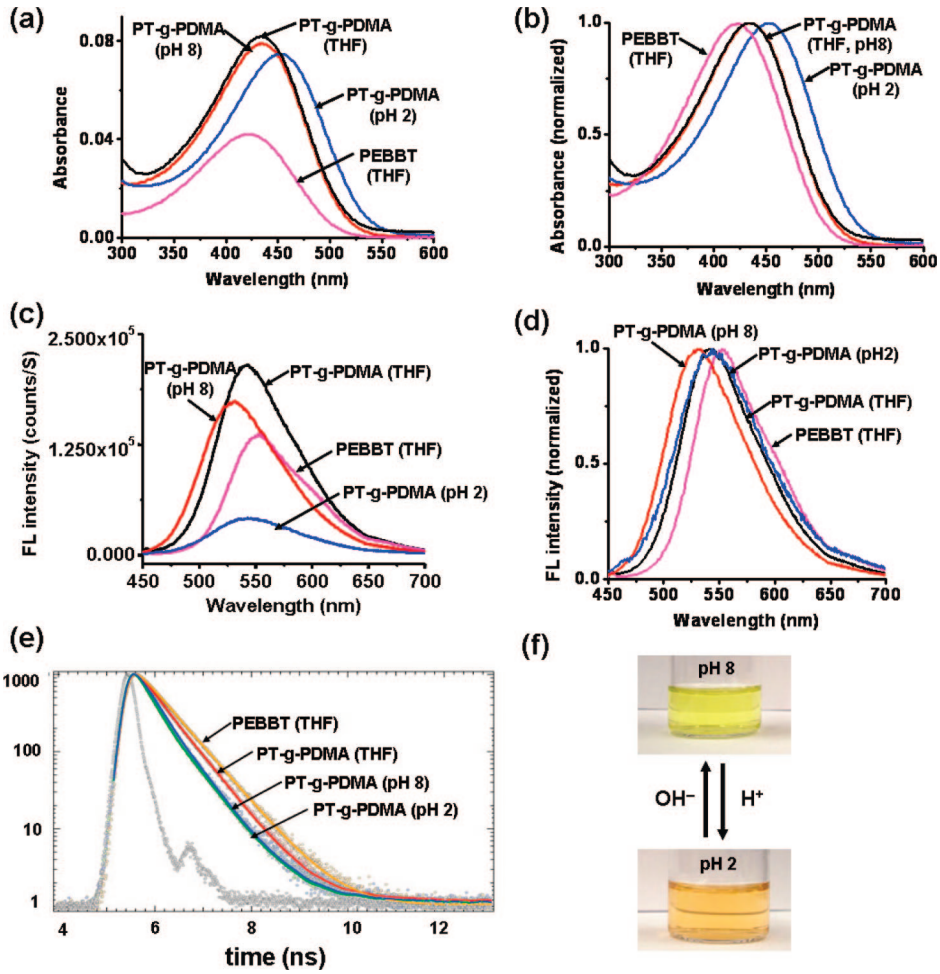

Figure 3. Absorption (a, b) and FL (c, d) spectra of PEBBT macroinitiator from in and PT-*g*-PDMA (0.1 g L^{-1}) in THF, in water at pH 8 and at pH 2. (b, d) Normalized absorption and FL spectra corresponding to (a) and (c), respectively. (e) Time-resolved FL decay profiles of these samples. A digital photograph of the polymer brush at pH 8 and pH 2 in water is shown in (f).

polymer in THF, a significant blue shift (ca. 13 nm, 56 meV) was observed for $\lambda_{max,em}$. In addition, there was a significant decrease of the average FL lifetime from THF (513 ps) to water (pH 8) (432 ps).

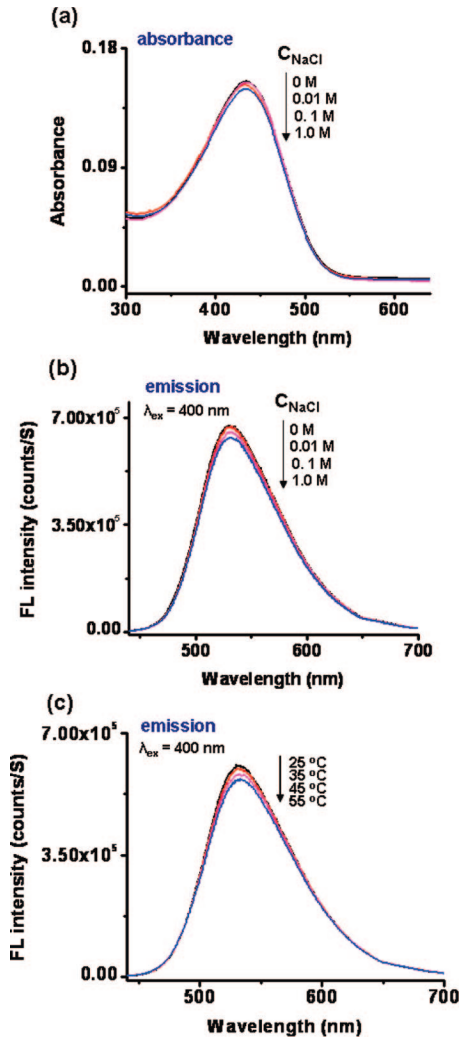

Figure 4. (a, b) Effect of the addition of different amounts of NaCl on the absorption (a) and FL (b) spectra of PT-*g*-PDMA (0.4 g L^{-1}, pH 8) in water. (c) Temperature dependence of the FL spectra of PT-*g*-PDMA in water (pH 8, 0.05 g L^{-1}).

We examined whether the PT-*g*-PDMA brushes can transduce the chemical information from the pH response of the PDMA side chains to the PT backbone. The natural pH of PT-*g*-PDMA in a 0.1 g L^{-1} aqueous solution is 8. At pH $\geq$ 8, the $\lambda_{max,abs}$ and $\lambda_{max,em}$ of PT-*g*-PDMA in water were 435 and 530 nm, respectively. There was no spectral shift with a pH increase from 8 to 12. With a decrease of pH from 8 to 2, we observed a gradual red shift for both $\lambda_{max,abs}$ (ca. 18 nm, 113 meV) and $\lambda_{max,em}$ (ca. 15 nm, 64 meV) (Figure 3a−d). The spectral red shift from pH 8 to 2 was accompanied by a dramatic decrease of the maximum FL intensity and a small decrease of the average FL lifetime from 432 to 409 ps, respectively, while the change of the polymer concentration was negligible. The onset of the spectral shift is in the range of pH = 7−8, i.e., near the reported pK_a of PDMA.[25] The pH responses of the absorption and FL spectra were reversible upon an increase of pH. The spectral shift from pH $\geq$ 8 to pH 2 led to a color change of the solution from yellow to dark orange (Figure 3d).

Concentration, Ionic Strength, and Temperature Effects. We then investigated whether other factors such as concentration, ionic strength, and temperature affect the spectroscopic properties of PT-*g*-PDMA polymer chains in aqueous solution. The results are shown in Figure 4. In these experiments, unbuffered polymer solutions at their natural pH (at 8) were used. Neither the absorption nor emission spectra showed any shift in the concentration range from 3 to 0.05 g L^{-1}. This result indicates that there is no significant conformational change of the PT backbone with the change of polymer concentration in aqueous solution.

To test the effect of ionic strength, we added various amounts of NaCl to the PT-*g*-PDMA solution while maintaining the polymer concentration at 0.4 mg/mL. The increase of [NaCl] from 0.01 to 1.0 M led to no shifts in the absorption or emission spectra. We monitored the FL spectra of PT-*g*-PDMA at 0.05 g L^{-1} in water at temperatures increasing from 25 to 55 °C. Only a slight decrease of the FL intensity was observed, with no shift of the wavelength of the maximal emission.

All these results indicate that the optical properties of PT-*g*-PDMA are relatively stable in water if the pH of the solution remains unchanged, e.g. at pH 8, implying that the PT backbone maintained its effective conjugation length over this range of concentrations, ionic strength, and temperature.

Solvent- and pH-Induced Conformational Changes of PT-*g*-PDMA in Solution. In this and the following sections of the paper, we describe experiments that provide information about the conformation of the PT-*g*-PDMA polymer in solution, in organic solvents, and in water at pH 2 and 8. Before presenting this information, we review briefly current ideas about the conformation of comb−graft copolymers in solution. There have been a number of theoretical studies. Many have examined the properties of these polymers in a common good (or Θ-) solvent for the backbone and the side chains.[28−32] These studies show that when the branch density is high, the backbone becomes elongated, and the polymer resembles a bottle-brush polymer (Scheme 2a). Borisov[33] recently examined a case more pertinent to our experiments, in which the polymer is in a good solvent for the side chains but a poor solvent for the backbone. Here the situation is more complex. Except at low grafting densities, the molecules do not aggregate because of the steric stabilization provided by the side chains. The tendency of the backbone to undergo collapse leads to several distinct compact structures. For high graft densities, the favored structure is a necklace of starlike micelles (Scheme 2b). When the solvent is extremely unfavorable for the backbone, there is evidence that polymer collapse into a spherical globule can occur (Scheme 2c). Nose's group[34,35] in Japan has reported detailed light scattering studies of a comb−graft copolymer in solvents selective for the side chains and for the backbone, with results in general accord with the picture presented above.

Atomic Force Microscopy (AFM) Characterizations. AFM is a powerful method for examining the conformational properties of comb-like grafted copolymers.[20,21,35−39] In this section, we describe tapping mode AFM together with light scattering experiments employed to investigate the structure of PT-*g*-PDMA in solution by examining differences in structure seen after deposition of samples onto mica. We compare results obtained with solutions in three different organic solvents and also examine the transition induced by the change of pH in water.

In Figure 5, we present representative height and phase contrast images of PT-*g*-PDMA samples on freshly cleaved mica obtained from dilute solutions (2×10^{-3} g L^{-1}) in three different organic solvents: toluene, THF, and dichloromethane. The bright wormlike features in the height images correspond to the PT backbones clad with PDMA side chains. The higher resolution images in Figures 5A,B display single molecules adsorbed on mica from dilute toluene solution. The molecules exhibit a characteristic corona morphology due to strong adsorption of PDMA side chains on the mica surface, which causes the flattening of side chains into lamellae with a thickness of 1.5 nm.[36,37] These corona features are less obvious for samples prepared from THF (Figures 5C,D) or CH_2Cl_2 (Figures 5E,F) solutions. This difference could be in part due to the short

Scheme 2. Proposed Model for the Conformational Transition of High-Density Comb−Graft Copolymers as a Function of $\chi_{s/backbone}$ in Bulk Solutions[a]

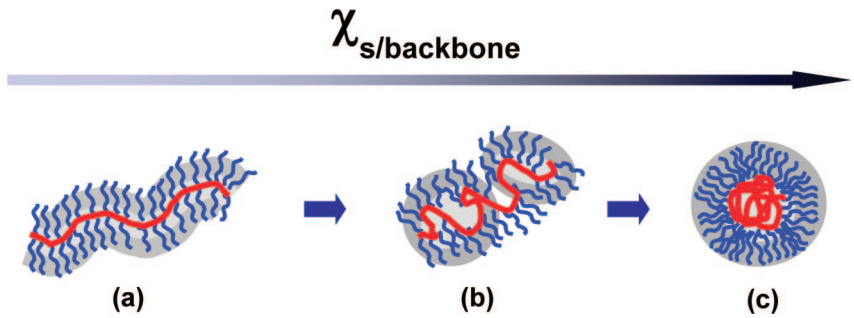

[a] The backbone collapses gradually with the increase of $\chi_{s/backbone}$ from left to right when the solvent becomes more and more poor for backbone while keeps good for the side chains. The repulsive steric interaction among the side chains prevents the multimolecular aggregation.

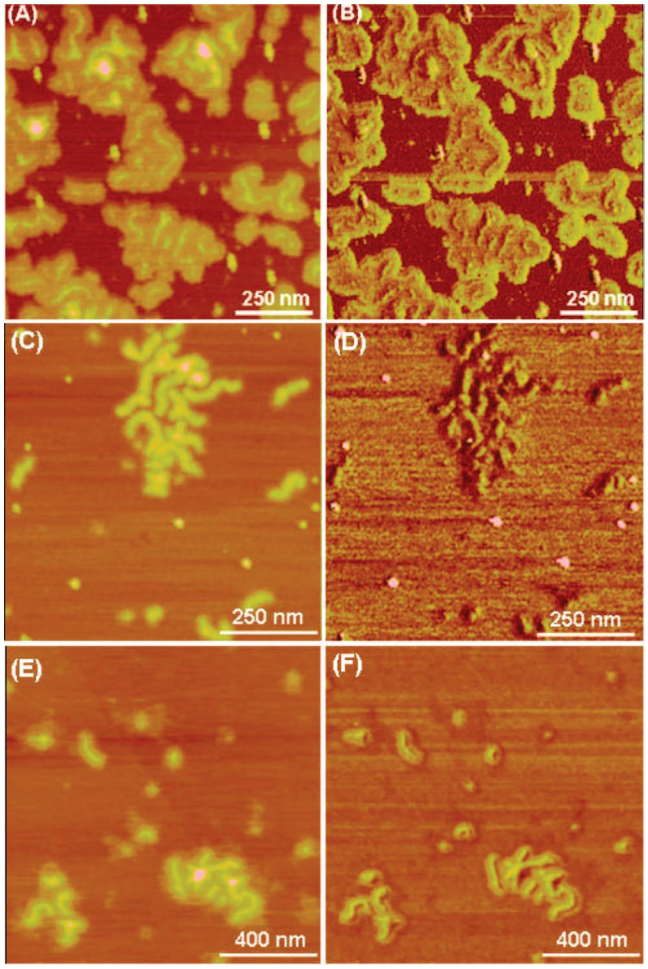

Figure 5. AFM images (A, C, E: height; B, D, F: phase) of PT-*g*-PDMA adsorbed on mica from dilute solution (2×10^{-3} g L^{-1}) of toluene (A, B), THF (C, D), and CH_2Cl_2 (E, F). Z range (height): 0−10 nm, from dark to bright.

adsorption period for the side chains of the polymers in solvents that evaporate much faster than toluene.[38] Nevertheless, wormlike feature and objects of similar size distribution can be seen for samples prepared from these three organic solvents. The elongated structures seen, for example, in Figures 5 A,B are consistent with the theoretical predictions for a densely grafted comb−graft copolymer in a good solvent for both the backbone and the side chains. The lengths of the wormlike cylinders in the AFM images vary from 50 to 200 nm.

A CONTIN plot from dynamic light scattering (DLS) measurements at 90° on a solution of PT-*g*-PDMA in THF (0.06 mg/mL) gave a broad monomodal peak with an apparent hydrodynamic radius $R_h^{app} = 43$ nm (Figure S5, Supporting Information). Similar measurements carried out at lower angles (60°, 30°) showed a shift of the peak to higher R_h^{app} values (64 nm at 60° and 89 nm at 30°). These data suggest the presence of a broad range of aggregates in solution, with the larger aggregates contributing more to the signal at low angles. Because large objects scatter light so much more intensely than smaller objects, it is possible that the aggregates that contribute to the DLS signal may be too few in number to be detected by microscopy measurements.

In Figure 6A−D, we present AFM images of PT-*g*-PDMA samples taken from aqueous solution at pH 2 and pH 8. Figures 6A,B show the AFM images of the sample (2×10^{-3} g L^{-1}) prepared at pH 2. One can see, in both the height and phase images, flower-like structures consisting of multiple segregated arms adjoining a smaller core with an average height of 1.9 ± 0.5 nm. For the sample prepared from a pH 8 aqueous solution under the same polymer concentration, one can discern well-defined backbones and pancake-like structures due to the side chains in both the height (Figure 6C) and phase (Figure 6D) images. All of the objects show characteristic white spots (high regions) in the centers surrounded by yellow-greenish regions with an average thickness of 1.3 ± 0.2 nm. The core is about 1.5 nm higher than the corona, with an average height of 2.3 ± 0.4 nm, slightly larger to that seen in the objects formed at pH 2. Zigzag features of the protruding edges are clearly distinguished in the phase image (Figure 6D).

In addition, the objects seen in the AFM images of PT-*g*-PDMA formed at pH 8 (Figures 6C,D) are significantly larger than those seen in images of the sample formed at pH 2 (Figures 6A,B). For example, for the samples prepared at pH 8, the widths of the elongated objects are on the order of 35−70 nm. The samples prepared at pH 2 yield structures that are more circular, with diameters in the range from 20 to 45 nm. In addition, for samples prepared at pH 8, many of the objects seen in the AFM images contain multiple cores (Figures 6C,D). This result suggests to us that the objects contain several polymer molecules.

The type of structures we see in these AFM images at pH 8 (Figures 6C,D) are similar to those reported by Müller et al.[39] They examined a somewhat different polymer brush with diblock copolymer arms [poly(acrylic acid)$_{39}$-*b*-poly(*n*-butyl acrylate)$_{118}$, (PAA-*b*-PnBA)] grafted from a backbone of poly(2-hydroxyethyl methacrylate)$_{240}$. They demonstrated that the core in the AFM images corresponded to PAA and the backbone of the brush, whereas the corona corresponded to the PnBA shell. In the case of our PT-*g*-PDMA brush, since water is a poor solvent for polythiophene and a much better solvent for PDMA side chains, we believe that the higher central cores in Figure

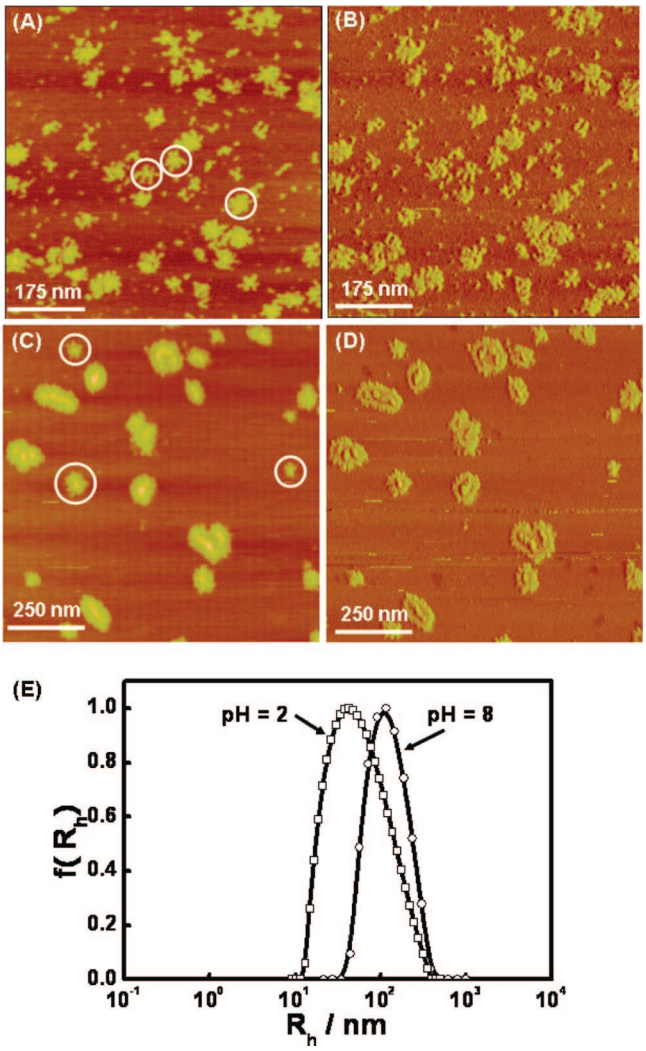

Figure 6. (A−D) AFM images (A, C: height; B, D: phase) of PT-*g*-PDMA adsorbed on mica from dilute aqueous solution (2×10^{-3} g L^{-1}) at pH 2 (A, B), and pH 8 (C, D). Z range (height): 5 nm (A); 8 nm (C). (E) CONTIN plots from 30° DLS measurements on the polymer brush (0.05 g L^{-1}) at pH 8 and pH 2. Circles in (A) and (C) point out objects assigned to single molecules of PT-*g*-PDMA. *Z* range (height): 0–5 nm for part A and 0–8 nm for part C, from dark to bright.

6C corresponds to the collapsed PT backbone. The flatter surrounding regions were formed by the PDMA side chains, which adhere strongly on mica.

Figure 6E shows CONTIN plots from 30° DLS measurements on PT-*g*-PDMA in water at pH 2 and pH 8. Both peaks are monomodal. The peak at pH 2 is somewhat broader (R_h^{app} = 46 nm (polydispersity 0.25)) and indicates that the species present are smaller than those present at pH 8. We attribute the peak at pH 2 primarily to the presence of individual molecules in solution. The shift of R_h^{app} to larger values (R_h^{app} = 95 nm (polydispersity 0.17)) at pH 8 is an indication that the molecules form finite-size aggregates in solution.

The pH-dependent change in radius seen in Figure 6 is reversible, as observed by absorption and fluorescence. In addition, when the pH value of the sample at pH 2 was increased back to pH 8 by adding 2.0 M NaOH, the molecular weight and polydispersity of this sample as measured by GPC were similar to those of the original sample at pH 8. Therefore, simple pH change does not lead to fragmentation of the macromolecule. The molecular weight obtained by GPC allows us to calculate the volume of the macromolecule when it is dry and on a surface, if we make the reasonable assumption that its density

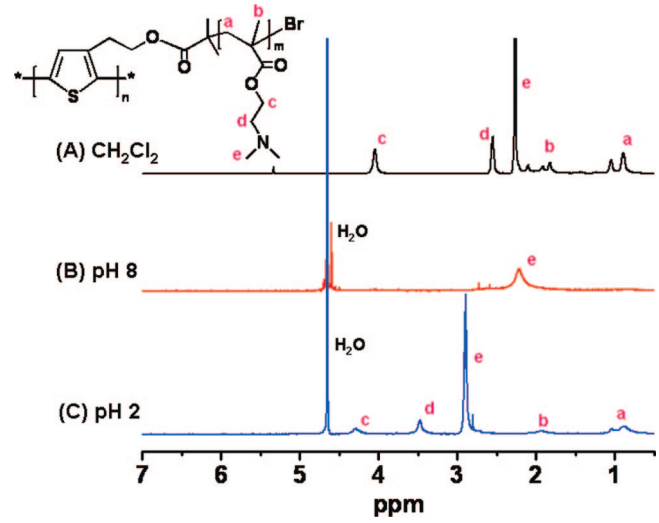

Figure 7. ^{1}H NMR spectra of PT-*g*-PDMA from CH_2Cl_2 (A) and aqueous solution at pH 8 (B) and pH 2 (C).

is ∼1 g/mL. This calculation indicates that the volume would be about 3000 nm^3, which corresponds roughly to several features circled in Figures 6A,C. This conclusion holds even if the molecular weight determined by GPC is off by a factor of 2. However, we note that in Figure 6A there are much smaller objects apparent on the surface. These are not contamination, and we conclude that they are fragments of the macromolecule generated by surface binding at low pH. There is a precedent for such adsorption-driven fragmentation,[40] but a detailed study of this observation is beyond the scope of this paper.

We attribute this size difference of PT-*g*-PDMA at these two pH values to the pH dependence of the solubility of PDMA in water. Water is a bad solvent for the polythiophene backbone, but PDMA ($pK_a \approx 7.5$) is strongly protonated in water at pH 2. Thus, water at pH 2 is a good solvent for these polycationic chains. We imagine that because of the polycationic chains, single molecules exist in solution, and these individual molecules adhere strongly to mica through ionic interactions. The degree of protonation of the PDMA side chains is much lower at pH 8. At pH 8, not only is water a poor solvent for the polythiophene backbone, it is a more marginal solvent for the PDMA brush. Our working model to explain the features of Figure 6 is that at pH 2 the solution consists primarily of individual molecules, and these deposit as molecules onto the mica substrate. At pH 8, the PT-*g*-PDMA forms colloidally stable aggregates consisting of relatively small numbers of polymer molecules. These contribute to the larger value of R_h^{app} in solution, and the clusters of molecules that form on the mica substrate and are detected by AFM (Figures 6C,D).

^{1}H NMR Experiments. ^{1}H NMR spectra provide evidence about the protonation of the PDMA side chains at low pH and about changes in chain mobility accompanying a change of solvent or pH. Examples are shown in Figure 7. In CD_2Cl_2, all the peaks from the PDMA side chains are well resolved. At pH 8 in water, the spectrum appears to be very simple, and only a broad peak from the dimethylamino protons can be seen. All other peaks of PT-*g*-PDMA have disappeared, presumably a consequence of restricted mobility of the PDMA side chains. In contrast, at pH 2, all of the peaks from the PDMA side chains appear again, consistent with enhanced mobility at low pH. As shown in Figure 7C, peaks c, d, and e of the $Me_2NCH_2CH_2O-$ groups are shifted downfield relative to their peaks in Figure 7A for the neutral polymer in CD_2Cl_2. These downfield shifts are a consequence of protonation of dimethylamino groups at pH 2.

Scheme 3. Proposed Mechanism for the Molecular Conformational Transition Accompanying the Change of Solvent Polarity or the Change of pH in Water

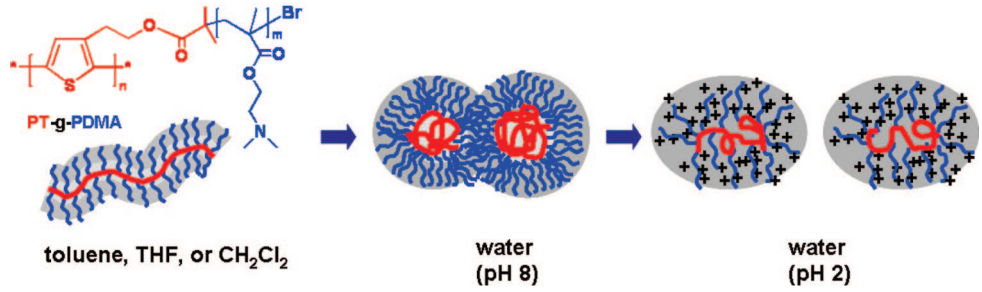

The ^{1}H NMR results indicate that the mobility of the PDMA side chains is restricted at pH 8 in water. We infer that this lack of mobility is a consequence of both intrachain and interchain association under relatively poor solvency conditions. These are also the conditions that would lead to intermolecular association (formation of aggregates), which we observed in AFM images such as those shown in Figures 6C,D. The reappearance and the shift of the proton peaks at pH 2 are consistent with the less compact structures and the lack of aggregation seen in the AFM image in Figures 6A,B.

Correlation between Optical Properties and Chain Conformation. Combining the results of AFM, light scattering, and ^{1}H NMR, we conclude that PT-*g*-PDMA forms an extended conformation in nonpolar organic solvents, such as toluene, THF, and CH_2Cl_2, all of which are good solvents for both the PT backbone and the PDMA side chains. AFM results indicate the rigid cylindrical structure in these nonselective solvents (such as THF), which is consistent with the theoretical prediction for such high-density, comb−graft copolymers. In water at pH 8, the PT backbones tend to aggregate to minimize their exposure to water, and the PDMA side chains form a more compact layer surrounding the PT backbone core. The conformational transition of the PT backbones from an extended chain in THF to a tighter and twisted chain coil in water (pH 8) is also consistent with the significant blue shift of (ca. 13 nm, 56 meV) $\lambda_{max,em}$ from THF to water (pH 8) (Figure 3), which indicates a decrease of the average conjugation length of the PT backbone. The ^{1}H NMR results show that the collapse of the PT backbones at pH 8 makes the PDMA side chains more crowded than in THF, leading to a significant decrease of side-chain mobility and to broad proton peaks. In addition, both DLS and AFM results indicate intermolecular bridging through the corona of PDMA chains. This type of aggregation can be explained by the relatively low solubility of PDMA in water at pH 8. The cores consisting of the collapsed PT backbones remain separated due to steric repulsion of the densely grafted side chains. This argument also explains why there is no spectra shift for PT-*g*-PDMA above pH 8.

In water at pH 2, protonation of the dimethylamino groups makes the PDMA side chains positively charged. Higher solubility and repulsion of the positively charged PDMA side chains tend to dissociate the bridging between PT-*g*-PDMA molecules and at the same time to stretch the PT backbone. As a consequence, the PT backbone is less folded and twisted at pH 2 than at pH 8, resulting in an increase of the average conjugation length and a red shift of both $\lambda_{max,abs}$ and $\lambda_{max,em}$. On the other hand, the PT backbone is hydrophobic and cannot form as extended a conformation in water as it does in toluene. The balance of these two effects results in the morphology of PT-*g*-PDMA seen in Figures 6A,B. A schematic representation of the conformational transitions of PT-*g*-PDMA from nonpolar organic solvents to water and that following the pH change from 8 to 2 are shown in Scheme 3.

Conclusion

We synthesized a polythiophene-based molecular brush (PT-*g*-PDMA) by growing PDMA chains from the PT backbone by ATRP. In dilute aqueous solution, the absorption and fluorescence spectra of the polymer brush show sensitive and reversible pH responses. We used AFM, light scattering, and ^{1}H NMR to investigate the conformational transitions of PT-*g*-PDMA with a change in pH that contribute to the spectral shifts. These results show that the polymer brush forms a more extended conformation with a decrease in pH from 8 to 2. Protonation of the Me_2N- groups and increased repulsive interactions among the PDMA side chains drive the red shift of the absorption and FL spectra of the PT backbone. Finally, we note that the good solubility of this polythiophene-based brush in a wide range of solvents is attractive for the fabrication of functional polymer composites. Moreover, PDMA as a cationic polymer has been utilized for gene delivery due to the favorable interaction with DNA. This opens the possibility of using the PT-*g*-PDMA polymer brush as a probe for DNA analysis.

Acknowledgment. This work was supported by NSERC Canada. We thank Dr. C. Vancaeyzeele for helpful discussions about the polythiophene synthesis.

Supporting Information Available: Digital photograph of PT-*g*-PDMA solutions in a variety of solvents, the normalized absorption and emission spectra of PT-*g*-PDMA in these solvents, GPC traces of PT-*g*-PDMA kept in dark in THF and the sample exposed to room light, section analysis of AFM images (height mode) of PT-*g*-PDMA from toluene as well as water at pH 8 and pH 2, respectively; plots of the maximum absorbances of PEBBT and PT-*g*-PDMA as a function of their weight concentrations in THF; autocorrelation functions and CONTIN plots from DLS measurements on PT-*g*-PDMA in THF at different angles; autocorrelation functions from DLS measurements on PT-*g*-PDMA in water at pH 8 and pH 2. This material is available free of charge via the Internet at http://pubs.acs.org.

References and Notes

(1) McQuade, D. T.; Pullen, A. E.; Swager, T. M. *Chem. Rev.* **2000**, *100*, 2537–2574.
(2) Friend, R. H.; Gymer, R. W.; Holmes, A. B.; Burroughes, J. H.; Marks, R. N.; Taliani, C.; Bradley, D. D. C.; Dos Santos, D. A.; Brédas, J. L.; Lögdlund, M.; Salaneck, W. R. *Nature (London)* **1999**, *397*, 121.
(3) Dennler, G.; Lungenschmied, C.; Neugebauer, H.; Sariciftci, N. S. *J. Mater. Res.* **2005**, *20*, 3224.
(4) Sirringhaus, H.; Tessler, N.; Friend, R. H. *Science* **1998**, *280*, 1741–1744.
(5) Liu, B.; Bazan, G. C. *Chem. Mater.* **2004**, *16*, 4467–4476.
(6) (a) Wang, Y.; Euler, W. B.; Lucht, B. L. *Chem. Commun.* **2004**, *686*, 687. (b) Matthews, J. R.; Goldoni, F.; Schenning, A. P. H. J.; Meijer, E. W. *Chem. Commun.* **2005**, *5503*, 5505.
(7) (a) McCullough, R. D.; Ewbank, P. C.; Loewe, R. S. *J. Am. Chem. Soc.* **1997**, *119*, 633–634. (b) Leclerc, M. *Adv. Mater.* **1999**, *11*, 1491–1498. (c) Ho, H. A.; Boissinot, M.; Bergeron, M. G.; Corbeil, G.;

Dore, K.; Boudreau, D.; Leclerc, M. *Angew. Chem., Int. Ed.* **2002**, *41*, 1548. (d) Ho, H. A.; Leclerc, M. *J. Am. Chem. Soc.* **2003**, *125*, 4412–4413. (e) Li, C.; Numata, M.; Takeuchi, M.; Shinkai, S. *Angew. Chem., Int. Ed.* **2005**, *44*, 6371–6374.
(8) Pinto, M. R.; Kristal, B. M.; Schanze, K. S. *Langmuir* **2003**, *19*, 6523–6533.
(9) Wang, F.; Bazan, G. C. *J. Am. Chem. Soc.* **2006**, *128*, 15786–15792.
(10) Schwarz, B. J. *Annu. Rev. Phys. Chem.* **2003**, *54*, 141–172.
(11) (a) Nguyen, T. Q.; Doan, V.; Schwartz, B. J. *J. Chem. Phys.* **1999**, *110*, 4068–4078. (b) Nguyen, T. Q.; Yee, R. Y.; Schwartz, B. J. *J. Photochem. Photobiol. A* **2001**, *144*, 21–30. (c) Nguyen, T. Q.; Schwartz, B. J. *J. Chem. Phys.* **2002**, *116*, 8198–8208.
(12) Bässler, H.; Schweitzer, B. *Acc. Chem. Res.* **1999**, *32*, 173–182.
(13) Barbara, P. F.; Gesquiere, A. J.; Park, S. -J.; Lee, Y. J. *Acc. Chem. Res.* **2005**, *38*, 602–610.
(14) Scholes, G. D.; Rumbles, G. *Nat. Mater.* **2006**, *5*, 683–696.
(15) Costanzo, P. J.; Stokes, K. K. *Macromolecules* **2002**, *35*, 6804–6810.
(16) Breen, C. A.; Deng, T.; Breiner, T.; Thomas, E. L.; Swager, T. M. *J. Am. Chem. Soc.* **2003**, *125*, 9942–9943.
(17) Wang, Y.; Erdogan, B.; Wilson, J. N.; Bunz, U. H. F. *Chem. Commun.* **2003**, *1624*, 1625.
(18) Balamurugan, S. S.; Bantchev, G. B.; Yang, Y.; McCarley, R. L. *Angew. Chem., Int. Ed.* **2005**, *44*, 4872–4876.
(19) Economopooulos, S. P.; Chochos, C. L.; Gregoriou, V. G.; Kallitsis, J. K.; Barrau, S.; Hadziioannou, G. *Macromolecules* **2007**, *40*, 921–927.
(20) Sheiko, S. S.; Möller, M. *Chem. Rev.* **2001**, *101*, 4099–4124.
(21) Gerle, M.; Fischer, K.; Roos, S.; Müller, A. H. E.; Schmidt, M.; Sheiko, S. S.; Prokhorova, S.; Möller, M. *Macromolecules* **1999**, *32*, 2629–2637.
(22) Phillips, D.; O'Connor, D. V. *Time Correlated Single Photon Counting*; Academic Press: London, 1984.
(23) McCullough, R. D. *Adv. Mater.* **1998**, *10*, 93–116.
(24) Cheng, G.; Bo1ker, A.; Zhang, M.; Krausch, G.; Müller, A. H. E. *Macromolecules* **2001**, *34*, 6883–6888.
(25) van de Wetering, P.; Zuidam, N. J.; van Steenbergen, M. J.; van der Houwen, O. A. G. J.; Bnderberg, W. J. M.; Hennink, W. E. *Macromolecules* **1998**, *31*, 8063–8068.
(26) Pantoustier, N.; Moins, S.; Wautier, M.; Degee, P.; Dubois, P. *Chem. Commun.* **2003**, *340*, 341.
(27) Heffner, G. W.; Pearson, D. S. *Macromolecules* **1991**, *24*, 6295–6299.
(28) Rouault, Y.; Borisov, O. V. *Macromolecules* **1996**, *29*, 2605–2611.
(29) Birshtein, T. M.; Borisov, O. V.; Zhulina, E. B.; Khokhlov, A. R.; Yurasova, T. A. *Polym. Sci. USSR* **1987**, *29*, 1293–1300.
(30) Borisov, O. V.; Birshtein, T. M.; Zhulina, E. B. *Polym. Sci. USSR* **1987**, *29*, 1552–1559.
(31) Fredrickson, G. *Macromolecules* **1993**, *26*, 2825–2831.
(32) Zhulina, E. B.; Vilgis, T. *Macromolecules* **1995**, *28*, 1008–1015.
(33) Borisov, O. V.; Zhulina, E. B. *Macromolecules* **2005**, *38*, 2506–2514.
(34) Kikuchi, A.; Nose, T. *Macromolecules* **1996**, *29*, 6770–6777.
(35) Kikuchi, A.; Nose, T. *Polymer* **1996**, *37*, 5889–5896.
(36) Beers, K. L.; Gaynor, S. G.; Matyjaszewski, K.; Sheiko, S. S.; Möller, M. *Macromolecules* **1998**, *31*, 9413–9415s.
(37) Neugebauer, D.; Zhang, Y.; Pakula, T.; Sheiko, S. S.; Matyjaszewski, K. *Macromolecules* **2003**, *36*, 6746–6755.
(38) Gerle, M.; Fischer, K.; Schmidt, M.; Roos, S.; Müller, A. H. E.; Sheiko, S. S.; Prokhorova, S. A.; Möller, M. *Macromolecules* **1999**, *32*, 2629–2637.
(39) Zhang, M.; Breiner, T.; Mori, H.; Müller, A. H. E. *Polymer* **2003**, *44*, 1449–1458.
(40) Sheiko, S. S.; Sun, F. C.; Randall, A.; Shirvanyants, D.; Rubinstein, M.; Lee, H.; Matyjaszewski, K. *Nature (London)* **2006**, *440*, 191–194.

MA800777M